JOURNAL OF MATERIALS SCIENCE 27 (1992) 4940–4944

Spherulite deformation at low strains in uniaxially extended polypropylene

T. ARIYAMA
Department of Mechanical Engineering, Faculty of Engineering, Science University of Tokyo, 1-3 Kagurazaka, Shinjuku-ku, Tokyo 162, Japan

The microscopic structure of uniaxially extended polypropylene (PP) at comparatively low strains was investigated by use of thermophotometry (TP) tests and polarizing microscopy. The spherulites for the uniaxially extended samples were deformed to an elliptic character with an increase in strains up to three, without the formation of the finer spherulites. The process of the spherulite deformation in the extended sample is different from that in hydrostatically extruded samples. The shape of TP curve in the extruded sample with a reduction cross-sectional area of 50% is fairly similar to that in the extended film with the strain of 1.0. The bulk strain was larger than the spherulite strain below the strain of 1.5. The results are explained in terms of the extension regions between the spherulites.

1. Introduction

The microscopic structure for hydrostatically extruded polypropylene (PP) has been investigated by use of polarizing microscopy and thermophotometry tests [1, 2]. The characteristic changes in the morphology of the spherulites of PP extrudates occurred at a percentage reduction in the cross-sectional area, R, of $R = 50\%$: the shape of the spherulites beyond $R = 50\%$ changed from spherulitic to elliptic. In addition, the behaviour of melting point as well as specific heat was related to marked changes in the spherulites and in the degree of crystallinity. Similar behaviour was also observed for the storage and loss moduli determined internal friction measurements [3]. Below $R = 50\%$, the β-loss peak increased in magnitude because of the increase in amorphous chains squeezed from the interior of the spherulites on hydrostatic extrusion; above $R = 50\%$, the β-loss peak overlapped with the α-loss peak because of the increase in strain chains [2]. Samuels [4] reported the spherulite deformation for uniaxially elongated films with extrusion ratios up to five at a testing temperature of 110 °C. He concluded from the small-angle light scattering measurements and the wide-angle X-ray diffraction analysis that the spherulites deformed affinely with the isotactic polypropylene films. Hence, for the uniaxially elongated sample, the spherulites deformed to the fibrillar structure without the formation of the finer spherulites, which were observed for the extrudates with $R = 50\%$ [1].

This study aimed to clarify the microscopic structure of uniaxially extended polypropylene samples at comparatively low strains by use of thermophotometry tests and polarizing microscopy. In addition, the sets of results were discussed on the basis of spherulitic deformation and were compared with those of spherulitic structure of the extrudates obtained by hydrostatic extrusion.

2. Experimental procedure

2.1. Materials

The polypropylene (PP) grade used in this work was Grade FA in the form of sheets, supplied by Futamura Chemical Co., Ltd. The spherulitic structure was the monoclinic α-form. The melt flow index was 5.5 g per 10 min (BS 2782 Method 10SC) and the apparent density was 0.908 g cm^{-3}.

For the materials for hydrostatic extrusion, the rod-like polypropylene from Ube Industries, Ltd., Grade J105 was used: crystal modification was the monoclinic α-form, the melt flow index was 5 g per 10 min, the apparent density was 0.907 g cm^{-3}, and the degree of crystallinity was 56% [1]. The molecular weight was 285000, estimated from the melt flow index. The average diameter of the spherulites in the original materials was 180 μm.

2.2. Preparation of samples

2.2.1. Uniaxially extended samples

The samples were obtained by heating the PP sheets *in vacuo* at 230 °C for 30 min followed by annealing at a cooling rate of 5 °C min^{-1}. The samples were then rolled at 80 °C. Hence, we obtained the 10 μm-thickness films with various strains up to three.

2.2.2. Hydrostatically extruded samples

Materials were machined to nosed billets with adequate diameter for various reductions in cross-sectional area R, up to $R = 80\%$

$$R(\%) = [1 - (d/D)^2] \times 100 \quad (1)$$

where d is the die outlet diameter of 9 mm and D the original billet diameter. The billets were hydrostatically extruded by a high pressure apparatus, with castor oil as a pressure-transmitting fluid, under

0022–2461

hydrostatic pressure up to 120 MPa. The semicone angle of the die was chosen to be 20° for every billet and the extrusion rate at the die exit was 5.3 mm s^{-1}. A detailed description of the extrusion procedure is given elsewhere [5]. Films of about 10 μm in thickness were microtomed from the extrudates parallel to the extrusion direction.

2.3. Thermophotometry tests

Fig. 1 shows a schematic of the device for thermophotometry (TP) tests, with an improvement of a polarizing microscope. The change in the intensity of light transmitting through a thin section of the samples was detected by means of a CdS cell. A hot stage was set on a revolving stage of the polarizing microscope. The sample was put directly on the heater composed of an electroconductive glass. The glass was coated with tin and metallic oxide. The TP tests were carried out at a heating rate of 2 °C min^{-1}.

2.4. Polarizing microscopy

The polarizing micrographs were obtained under two experimental conditions: a constant extrusion rate of 1.6 mm min^{-1} at a testing temperature of 120 °C and a constant load extension of 4.7 MPa.

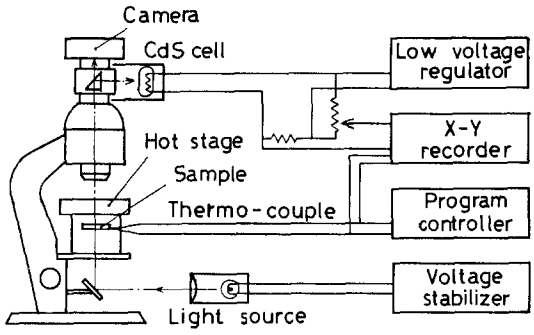

Figure 1 Schematic of device for thermophotometry tests.

3. Results and discussion

3.1. Spherulitic deformation

Fig. 2 shows the typical photographs obtained by polarizing microscopy for both the uniaxially extended samples and the hydrostatically extruded samples. As shown in Fig. 2a and d, the spherulites of the α-form structure were observed with a spherulite diameter of approximately 100 μm; the amorphous parts were also observed between the spherulites. The shape of spherulites changed from spherical to elliptic in the extrudates above $R = 50\%$. In addition, no amorphous regions between the deformed spherulites were observed at $R = 60$–80%. In particular, the spherulites with $R = 50\%$ changed from coarse structure to a finer one by an imposition of hydrostatic pressure.

On the contrary, the spherulites for the uniaxially extended samples were deformed to an elliptic (or an egg-shaped) character with an increase in strains up to three, without the formation of the finer spherulites; in particular, the amorphous regions between the spherulites were not observed for the films with strains above $\varepsilon = 1.4$. The process of the spherulitic deformation in the extended samples is significantly different from that in the hydrostatically extruded samples.

Table 1 shows the ratio R_d and the ratio R_n for the extended films and the extruded samples: R_d is the ratio of the length of major axis to that of minor axis of spherulites; R_n is the ratio of the length of major axis to the distance between the center of spherulites. R_d of the extrudates increased gradually with increasing R, but R_n decreased up to $R = 40\%$. On the

TABLE I Properties of spherulites

Extrudates			Extended films		
R, %	R_d	R_n	ε	R_d	R_n
0	1.0	1.0	0	1.0	0.9
30	1.2	0.7	0.5	1.4	0.9
40	1.4	0.7	1.0	1.6	1.0
50	1.9	1.0	1.4	2.0	1.2
60	2.5	1.1	2.0	2.1	1.3
70	3.1	1.2	2.5	2.2	1.3

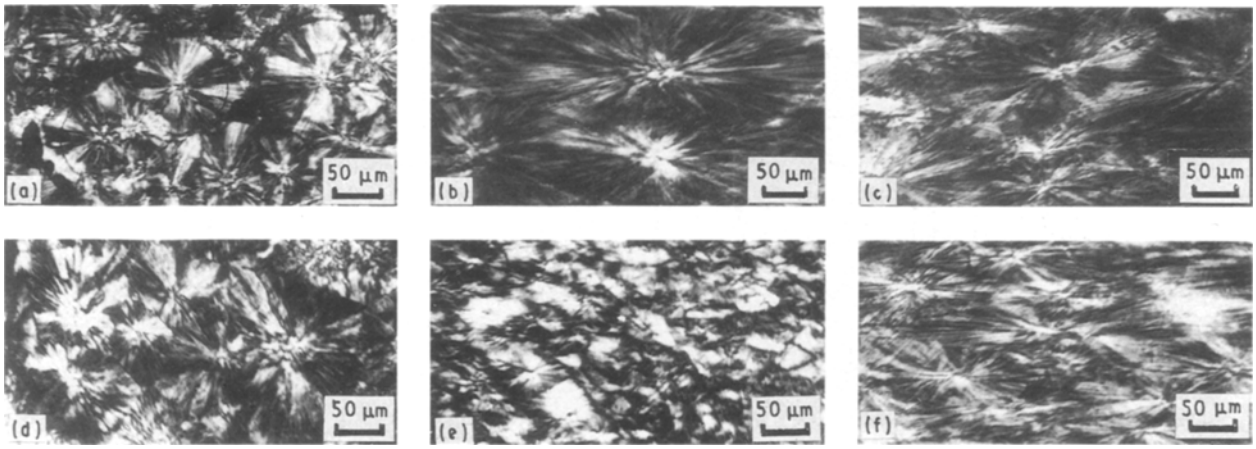

Figure 2 Polarizing micrographs of uniaxially extended PP films: (a) $\varepsilon = 0$, (b) $\varepsilon = 1.4$, (c) $\varepsilon = 2.0$, (d) $R = 0\%$, (e) $R = 50\%$, (f) $R = 70\%$ and of PP extrudates parallel to the extrusion direction.

contrary, both R_d and R_n in the extended films increased with increasing strain ε. The deformation mechanism for the extended films is the same as for the extruded samples, except for the extrudates below $R = 50\%$. The value of $R_n = 1.0$ means that the spherulites were in contact with each other to the draw direction at the outer zones of the adjacent spherulites. Accordingly, beyond $R_n = 1.0$ the spherulites were deformed to elliptic.

3.2. Light transmitting intensity

Fig. 3 shows the light transmitting intensity versus temperature obtained by means of TP tests in the uniaxially extended samples and the hydrostatically extruded samples. The spherulitic deformation behaviour was confirmed by the direct observation with naked eye when the sample was heated at 2 °C min^{-1}. The intensity curve in the extended film with strain $\varepsilon = 0$ is fairly different from that in other TP curves: the small peak observed at about 154 °C, which is indicated by an arrow in Fig. 3a, is attributed to the melt of β-crystals. This peak is gradually reduced in intensity with an increase in strain ε; this peak disappears in the extended films with $\varepsilon = 1.5$. In the extended films above $\varepsilon = 2$, a single peak only is observed; this peak is attributed to the melt of α-crystals. The resulting behaviour exhibiting the single peak in the extended films is basically identical to that in the extruded samples. The shape of the TP curve in the extruded sample with $R = 50\%$ is very similar to that in the extended film with $\varepsilon = 1.0$. Since the amount of strain of $\varepsilon = 1.0$ corresponds to $R = 50\%$ (R_d values in Table 1), the value of $\varepsilon = 1.0$ (or $R = 50\%$) gives a critical number. In fact, the deformation mechanism in the extrudates produced by hydrostatic extrusion was divided in two stages below and above $R = 50\%$ [1].

Fig. 4 shows the ratio of light intensity R_i in both the extended films and the extruded samples, together with the melting temperature T_{mp}, defined as the end-off temperature at which the light intensity levels off. R_i in the extended films remained constant at 1.0 at the strain range of $\varepsilon = 0$–1.0. In addition, R_i in both

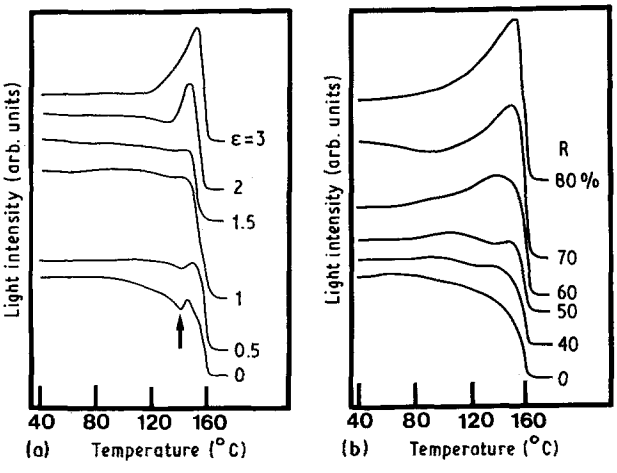

Figure 3 Light transmitting intensity versus temperature for PP (a) uniaxially extended films; (b) extrudates parallel to the extrusion direction.

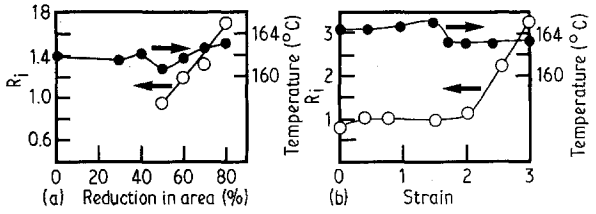

Figure 4 Effect of strain (a) and reduction in area (b) on the ratio $[R_i]$ of light intensity, along with the melting temperature $[T_{mp}]$: $R_i = I/I_0$; I is the intensity at a peak temperature, I_0 is the intensity at room temperature.

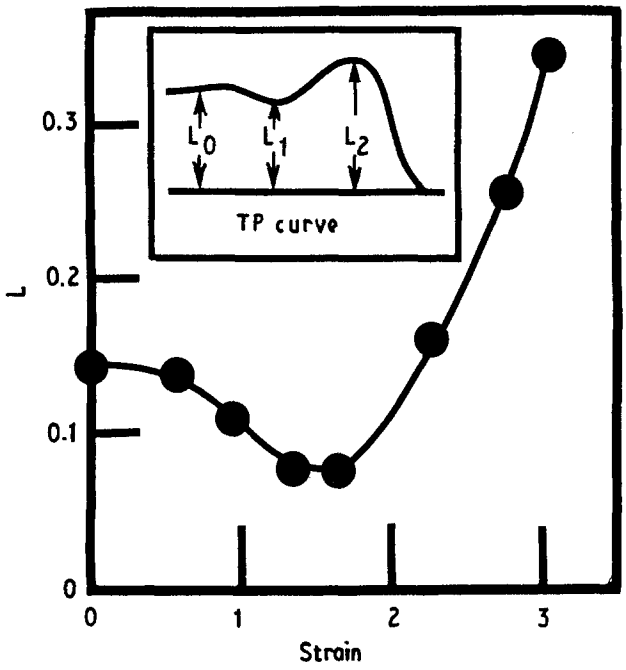

Figure 5 Light intensity $[L]$ versus strain: $L = (L_2 - L_1)/L_0$.

samples indicated similar behaviour above $\varepsilon = 1.0$ (or $R = 50\%$); both R_i increased with increasing strain ε and reducing R.

3.3. Deformation under constant rate extension

Fig. 5 shows the light intensity L under a constant rate of extension of 1.6 mm min^{-1} at 120 °C. The light intensity L in the extended films was a minimum at $\varepsilon = 1.5$. Small values of L mean small changes in the molecular chains. Thus, the extended films with $\varepsilon = 1.2$–1.5 indicated the smallest change of molecular chains including the spherulites.

Fig. 6 shows the polarizing micrographs of the extended films with different strains under a constant rate extension. In the samples with $\varepsilon = 0$ (Fig. 6a and b), necking occurred at the parts of atactic chains between the spherulites. As shown in Fig. 6b, at elongation = 15%, atactic parts were observed in the interior of the spherulites; this part has been presented at elongation = 0% (Fig. 6a). Thus, necking deformation is concentrated on the outer zones of the weak spherulite boundaries. On the contrary, the sample with $\varepsilon = 1.4$ was elongated homogeneously to the

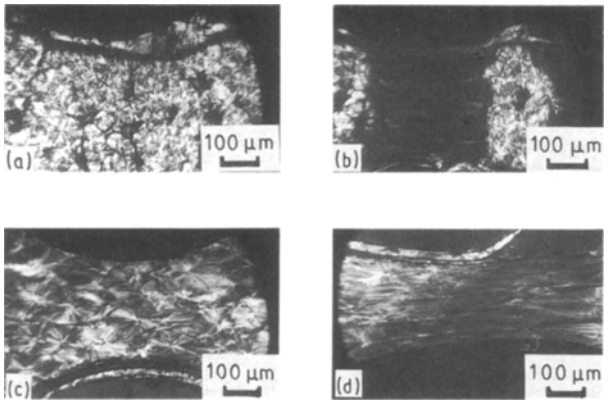

Figure 6 Polarizing micrographs under an extension ratio of 1.6 mm min^{-1} at 120 °C. ε = 0 (a) elongation = 0%, (b) elongation = 15%, ε = 1.4 (c) elongation = 0%, (d) elongation = 15%.

extension direction without necking (Fig. 6c and d) and the spherulites were oriented parallel to the draw direction. Similar spherulite deformation was also observed in the sample with strains above ε = 1.4 up to ε = 3.0.

Fig. 7 shows the spherulite strain versus bulk strain in the uniaxially extended films. The spherulite strain is defined as the spherulite size parallel to the extension direction, determined by direct observations of a polarizing microscope; on the other hand, the bulk strain is the elongation of the gauge length in the thin film and gauge section was continually photographed during the tests. As shown in Fig. 7, the experimental points fit approximately the predicted line for an affine deformation of the spherulites. However, from the precise observation, the bulk strain was larger than the spherulite strain below ε = 1.5: the results are explained in terms of an extension of amorphous regions between the spherulites.

3.4. Deformation under constant load extension

Fig. 8 shows the temperature versus strain in uniaxially extended films under a constant load extension of 4.7 MPa at a heating rate of 2 °C min^{-1}. The melting temperature, the temperature at 32% elongation, and the temperature at an initial deflection in TP curves are the minimum at approximately ε = 1.5. This behaviour is fairly similar to that of light intensity under the constant rate extension. The value of ε = 1.5 is a characteristic figure in both the deformations under constant rate extension and under constant load extension. Since the completion of crystallization in the parts of atactic chains occurs at strain of ε = 1.5, the spherulite or molecular chains become soft.

4. Conclusion

The microscopic structure of uniaxially extended polypropylene at comparatively low strains was studied by use of thermophotometry tests and polarizing microscopy. The sets of results were compared with those of spherulitic structure of the extrudates obtained by hydrostatic extrusion. The shape of spherulites changed from spherical to elliptic in the extrudates above R = 50%: in particular, the spherulites with R = 50% changed from coarse structure to finer one

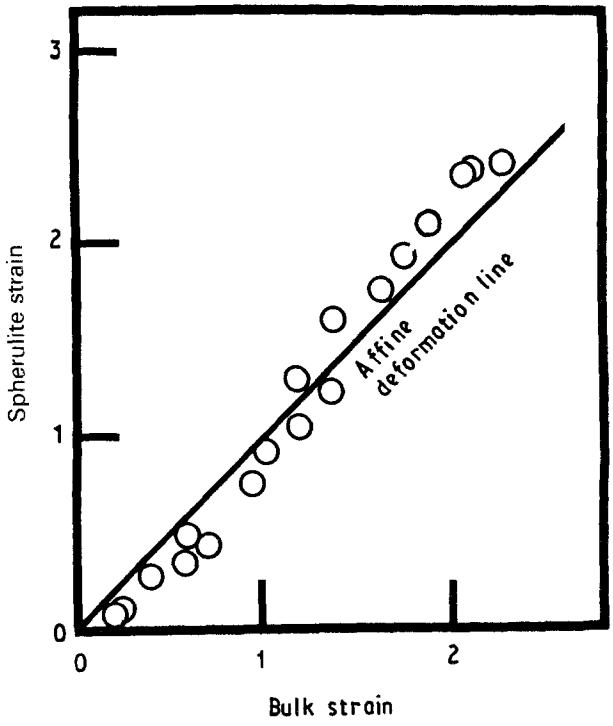

Figure 7 Spherulite strain versus bulk strain for uniaxially extended films.

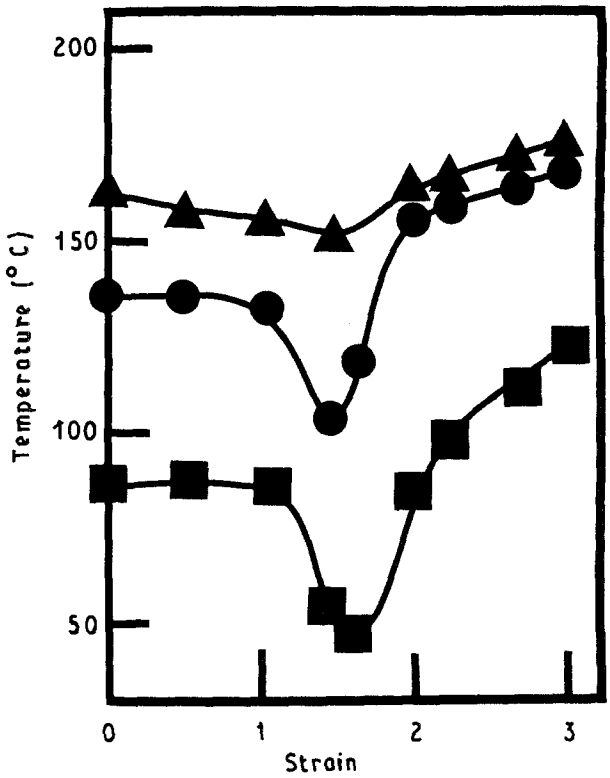

Figure 8 Temperature versus strain: (▲) melting temperature; (●) temperature at 32% elongation; (■) temperature of initial deflection of curve.

by an imposition of hydrostatic pressure. On the contrary, the spherulites for the uniaxially extended samples were deformed to an elliptic (or egg-shaped) character with an increase in strains up to three, without the formation of the finer spherulites. The process of the spherulitic deformation in the extended samples is significantly different from that in the hydrostatically extruded samples.

The shape of TP curve in the extruded sample with $R = 50\%$ is very similar to that in the extended sample with $\varepsilon = 1.0$. Since the value of strain of $\varepsilon = 1.0$ corresponds relatively to $R = 50\%$, the value of $\varepsilon = 1.0$ gives a critical number. From the polarizing micrographs obtained under constant rate extension, in the samples with $\varepsilon = 0$, necking occurred at the parts of atactic chains between the spherulites. The necking deformation is concentrated on the outer zones of the weak spherulite boundaries. On the contrary, the sample with $\varepsilon = 1.4$ was elongated homogeneously to the extension direction without necking and the spherulites were oriented parallel to the draw direction.

The bulk strain was larger than the spherulite strain below $\varepsilon = 1.5$: this result is explained in terms of the extension of amorphous regions between spherulites.

Acknowledgements

The author is indebted to Dr M. Takenaga for helpful discussion throughout these studies and also to Profs K. Yamagata, A. Kasai, and N. Inoue for encouragement and suggestions.

References

1. T. ARIYAMA, M. TAKENAGA, T. TSUCHIYA, and K. YAMAGATA, *Rept. Prog. Polym. Phys. Jpn* **30** (1987) 177.
2. T. ARIYAMA, M. TAKENAGA, T. NAKAYAMA, K. YAMAGATA, and N. INOUE, *ibid.* **30** (1987) 337.
3. T. ARIYAMA, M. TAKENAGA, K. YAMAGATA, T. TSUCHIYA, and N. INOUE, *ibid.* **31** (1988) 305.
4. R. J. SAMUELS, *J. Polym. Sci. A* **3** (1965) 1741.
5. N. INOUE, T. NAKAYAMA, T. ARIYAMA, *J. Macromol. Sci. Phys.* **B19** (1981) 543.

Received 14 May
and accepted 20 September 1991